Histol Histopathol (2022) 37: 655-664

http://www.hh.um.es

Histology and Histopathology
From Cell Biology to Tissue Engineering

ORIGINAL ARTICLE **Open Access**

Class II lupus nephritis with podocyte injury in imiquimod-induced lupus-prone mice

Atsuko Murai[1], Masaki Yamazaki[1], Kaori Nishihara[1], Aki Kito[2], Sohei Oyama[2], Naoshi Horiba[2] and Atsuhiko Kato[1]

[1]Translational Research Division and [2]Research Division, Chugai Pharmaceutical Co., Gotemba, Shizuoka, Japan

Summary. Lupus nephritis (LN) is a renal disease presented in systemic lupus erythematosus (SLE) and is divided into 6 classes based on histopathological criteria set by the International Society of Nephrology/Renal Pathology Society. Major mouse models of SLE usually develop class III/IV LN, which are characterized by subendothelial deposits and endocapillary hypercellularity. We examined the pathological features of kidneys in a mouse model of SLE induced by a toll-like receptor 7 agonist, imiquimod (IMQ). In experiment 1, eleven-female FVB/NJcl wild type mice were treated with IMQ on their ear skin 3 times per week. Plasma anti-dsDNA increased from 2 weeks after first IMQ treatment and 2 mice exhibited nephrotic syndrome from 6 weeks. Histopathology revealed eosinophilic mesangial deposits in all mice from 4 weeks. Subsequently, podocytes showed enlargement with vacuolation and their numbers decreased in 6 mice. There was no infiltration of inflammatory cells, subendothelial deposits in glomeruli, or subepithelial deposits in glomeruli. In experiment 2 using 10 mice at 8 weeks after IMQ treatment, the mesangial deposits were observed in all mice and confirmed to be IgG, IgA, IgM, C1q and C3 by immunofluorescence, which corresponds to class II LN. Foot process effacement was detected by transmission electron microscopy and was considered to lead to proteinuria. These mice exhibited pathological characteristics corresponding to class II LN and podocyte injury, which make it distinct from other mouse models of SLE.

Key words: Lupus nephritis, Imiquimod, TLR 7, Mice

Corresponding Author: Atsuko Murai, Translational Research Division, Chugai Pharmaceutical Co., Ltd., 1-135 Komakado, Gotemba, Shizuoka, 412-8513, Japan. e-mail: murai.atsuko79@chugai-pharm.co.jp

DOI: 10.14670/HH-18-450

Introduction

Systemic lupus erythematosus (SLE) is an autoimmune disease characterized by the production of autoantibody that targets nuclei. It affects many organs, including kidney, joint, skin, and nervous system (Lech and Anders, 2013; Pedersen et al., 2015; Zhuang et al., 2015; Chen and Hu, 2018). Lupus nephritis (LN), a renal lesion associated with SLE, affects 30 to 70 % of SLE patients and has a negative impact on their prognosis (Sakhi et al., 2019; Gasparotto et al., 2020). The most widely adopted classification of LN was developed by the International Society of Nephrology/Renal Pathology Society (ISN/RPS). LN is divided into six classes based on the location of immune complex (IC) deposits and histopathological findings in kidney (Weening et al., 2004; Bajema et al., 2018). In class I LN, the IC deposits are localized in the mesangial area and can be detected by electron microscopy or immunofluorescence (IF), but not by light microscopy. Class II shows mesangial IC deposits with mesangial hypercellularity. Subendothelial deposits and endocapillary hypercellularity are characteristics of class III (<50% of all glomeruli) and IV (≥50% of all glomeruli). Class V shows membranous nephropathy characterized by subepithelial IC deposits, and class VI shows glomerular sclerosis in ≥90% of all glomeruli (Weening et al., 2004; Bajema et al., 2018). The prognosis differs based on the classification. The most severe prognosis with the highest risk of end stage renal disease is with class III and IV (Anders and Fogo, 2014; Sakhi et al., 2019; Gasparotto et al., 2020), where inflammatory response occurs in glomeruli (Sakhi et al., 2019). By contrast, classes I and II have a favorable prognosis (Anders and Fogo, 2014; Gasparotto et al., 2020).

NZB/NZWF1, MRL/lpr, and BXSB male mice function as major models of spontaneous SLE that are high in autoantibodies, including anti-dsDNA. They develop nephritis within 3-5 months and 50% of animals die at 6-15 months (Grande, 2011; Zhuang et al., 2015; Richard and Gilkeson, 2018). Their histopathological characteristics in kidney correspond to class III/IV LN;

these characteristics are diffuse proliferative glomerulonephritis in NZB/NZWF1 and MRL/lpr mice (Grande, 2011) and membranous proliferative glomerulonephritis with podocyte injury in BXSB male mice (Kimura et al., 2013). As for the induced model of SLE, pristane, an isoprenoid alkane, induces IC-mediated nephritis in BALB/c mice 6 months after intraperitoneal injection and the resulting glomerular lesions are consistent with class III/IV and V LN (Satoh et al., 1995; Zhuang et al., 2015). Imiquimod (IMQ), a toll-like receptor 7 (TLR7) agonist, also induces production of autoantibodies and lupus-like immune disease in wild type mice in a shorter time period than in other models, and was recently established by Yokogawa, et al. in 2014 (Yokogawa et al., 2014). Four week application of IMQ on ear skin leads to lupus-like disease in multiple organs, namely kidney, liver, heart and skin (Yokogawa et al., 2014). An intraperitoneal injection of IMQ accelerates the formation of glomerular lesions in a spontaneous lupus model and increases IL-12p70, IFN-α, IL-6, and glomerular IC deposits (Pawar et al., 2006).

TLR7 is expressed in plasmacytoid dendritic cells, macrophages, and B cells (Eleftheriadis et al., 2012; Lech and Anders, 2013; Zhuang et al., 2015). Usually, self DNA and RNA are not recognized by TLRs, whereas they are recognized as virus in SLE patients (Eleftheriadis et al., 2012; Lech and Anders, 2013). TLR7 activation promotes type I interferon production in the SLE (Zhuang et al., 2015; Sakata et al., 2018). Over-production of type I interferon seems to delay phagocytosis of apoptotic cells and activate B cells (Zhuang et al., 2015). The interferon signature is low or mild in most spontaneous SLE models, whereas it is high in pristane- (Zhuang et al., 2015) and IMQ-induced models (Yokogawa et al., 2014).

Although IMQ treatment is known to induce LN-like disease (Yokogawa et al., 2014), the details of these pathological changes are still not well understood. The present study was conducted to elucidate these pathological changes and compare them to those in human LN. Our data revealed that kidney changes in the IMQ-induced model correspond to class II LN with podocyte injury.

Materials and methods

Animals and treatment

All animals were handled in accordance with Guide for the Care and Use of Laboratory Animals at Chugai Pharmaceutical Co., Ltd., and all experimental protocols were approved by the Institutional Animal Care and Use Committee. Female FVB/NJcl mice were purchased from CLEA Japan, Inc. (Tokyo, Japan) and used at 6-8 weeks old. Sixteen mice (n=2-3 imiquimod-treated and 1 control mouse once every 2 weeks from 2 to 10 weeks after IMQ treatment) were used in Experiment 1 and 13 mice (n=10 imiquimod-treated and 3 control mice) were used in Experiment 2. The mice were treated with 5% IMQ cream (Mochida Pharmaceutical Co., Ltd, Tokyo, Japan) as previously described (Yokogawa et al., 2014). Briefly, 1.25 mg/head of IMQ cream was applied to the skin of the right ear 3 times per week. Control mice were not treated with IMQ. Samples were collected from all live animals to measure plasma anti-dsDNA and urine protein and were collected at necropsy to measure plasma albumin. The mice were euthanized by exsanguination under anesthesia and blood and kidneys were collected. To examine the time-course change, the samples from two or three mice treated with imiquimod and one without imiquimod were collected once every 2 weeks from 2 to 10 weeks after IMQ treatment in Experiment 1. For detailed glomerular analysis, all samples were collected at 8 weeks after IMQ treatment in Experiment 2.

Serological and urinary analysis

Plasma anti-dsDNA IgG autoantibody was measured using a mouse anti-dsDNA ELISA kit (Fujifilm Wako Shibayagi Corporation, Gunma, Japan). Levels of urinary protein, urinary creatinine, and plasma albumin were determined using the assay kits (Fujifilm Wako Pure Chemicals, Osaka, Japan). The protein-to-creatinine ratio was calculated by dividing the urinary protein excretion by the urinary creatinine excretion.

Histopathological analysis

Kidneys were fixed in 10% neutral buffered formalin (NBF) or Methyl Carnoy's fixative, embedded in paraffin. The sliced sections of NBF-fixed kidneys were stained with HE. Those fixed in Methyl Carnoy's were stained with periodic acid-Schiff and periodic acid methenamine silver for the histopathological analysis of glomeruli. Histopathological findings on glomeruli were graded as follows. Eosinophilic mesangial deposits were graded according to the severity: minimal, a low to moderate amount of deposits were found in each glomerulus in less than 50% of glomeruli; moderate, a low to moderate amount of deposits were found in each glomerulus in more than 50% of glomeruli; severe, deposits were found in almost all glomeruli with an especially high amount in more than 50% of them. Other findings were recorded as present or not present.

Immunohistochemistry (IHC) and IF

For IHC, the sliced sections of kidneys, which were fixed in 10% NBF and embedded in paraffin, were stained with antibodies against p57 Kip2 (1:1600; PA5-16539, Thermo Fisher Scientific, Waltham, MA), Ly-6G (1:200; #127602, BioLegend, San Diego, CA), F4/80 (1:400; MCA497, Bio-Rad, Hercules, CA), CD3 (1:100; ab16669, Abcam, Cambridge, UK) (Moroki et al., 2021), and CD19 (1:800; #90176, Cell signaling technology, Danvers, MA), followed by incubation with

horseradish peroxidase-conjugated anti rat-IgG or rabbit-IgG and visualized with diaminobenzidine and hematoxylin as counterstaining. P57 Kip2 was used as a podocyte marker as described in a previous study (Maeda et al., 2019). To examine the number of podocytes and inflammatory cells in glomeruli, 30 glomeruli were randomly selected and the numbers of cells positive with p57 Kip2, Ly-6G, F4/80, CD3, and CD19 were counted by pathologists and the results were expressed as means. For IF to detect IC deposits in glomeruli, kidneys were embedded in O.C.T. compound (Sakura Finetek Japan Co., Ltd, Tokyo, Japan) and were frozen. The sliced sections were fixed in 4% paraformaldehyde and stained with IgG (1:1000; ab190475, Abcam), IgA (1:400; ab97231, Abcam), Alexa Fluor 488-conjugated IgM (1:2000; A-21042, Thermo Fisher Scientific), C3 (1:180; ab200999, Abcam), and C1q (1:40; HM1044, Hycult Biotech, Uden, Netherlands) followed by staining with DyLight 488-conjugated secondary antibodies (Bethyl Laboratories, Inc., Montgomery, TX) excluding IgM. The sections were analyzed by fluorescence microscopy (Nikon Corporation, Tokyo, Japan).

Transmission Electron Microscopy (TEM)

Small pieces of kidneys were fixed with 0.5% glutaraldehyde (TAAB Laboratories Equipment Ltd, Berkshire, UK) and 1.5% paraformaldehyde (Electron Microscopy Sciences, Hatfield, PA) in 0.1 M phosphate buffer (Nakalai Tesque, Kyoto, Japan), followed by fixing with 1% osmium tetroxide (Nisshin EM Co., Ltd., Tokyo, Japan) and dehydrated by graded alcohol. The kidneys were embedded in epoxy resin. Ultrathin sections were stained with uranyl acetate and lead citrate and were observed under a transmission electron microscope (JEM-1400; JEOL Ltd., Tokyo, Japan).

Statistical analysis

Data on the number of Ly-6G, F4/80, CD3, and CD19 were expressed as the mean ± SEM. Comparisons between IMQ treatment groups and control were performed with Student's t-test. $p<0.05$ was considered statistically significant.

Results

Time-course analysis of IMQ treated mice

In IMQ-treated mice of Experiment 1, plasma anti-dsDNA IgG was increased from 2 weeks and reached peak 6 weeks after IMQ treatment compared with control mice (Fig. 1A). In 4 mice, urine protein/creatinine levels were markedly increased at levels over 100 (Fig. 1C) with decreased plasma albumin (Fig. 1B) from 6 weeks after IMQ treatment. In the histopathological analysis, eosinophilic mesangial deposits were observed in all mice, which appeared from 4 weeks after IMQ treatment (Table 1, Fig. 2B,F) and increased with long-term treatment (Table 1, Fig. 2C,D,G,H). These glomerular changes corresponded to those of class II LN and there were no findings suggestive of class III-V LN, such as endocapillary hypercellularity, capillary wall double contours, wireloop lesions, or subepithelial spikes (Weening et al., 2004; Anders and Fogo, 2014; Bajema et al., 2018). Enlargement of podocytes, vacuolation of podocytes/parietal epithelial cells, and hypertrophy and/or hyperplasia of parietal epithelial cells were detected in 6 mice from 6 weeks after IMQ treatment (Table 1, Fig. 2D,H). The mice exhibiting symptoms of

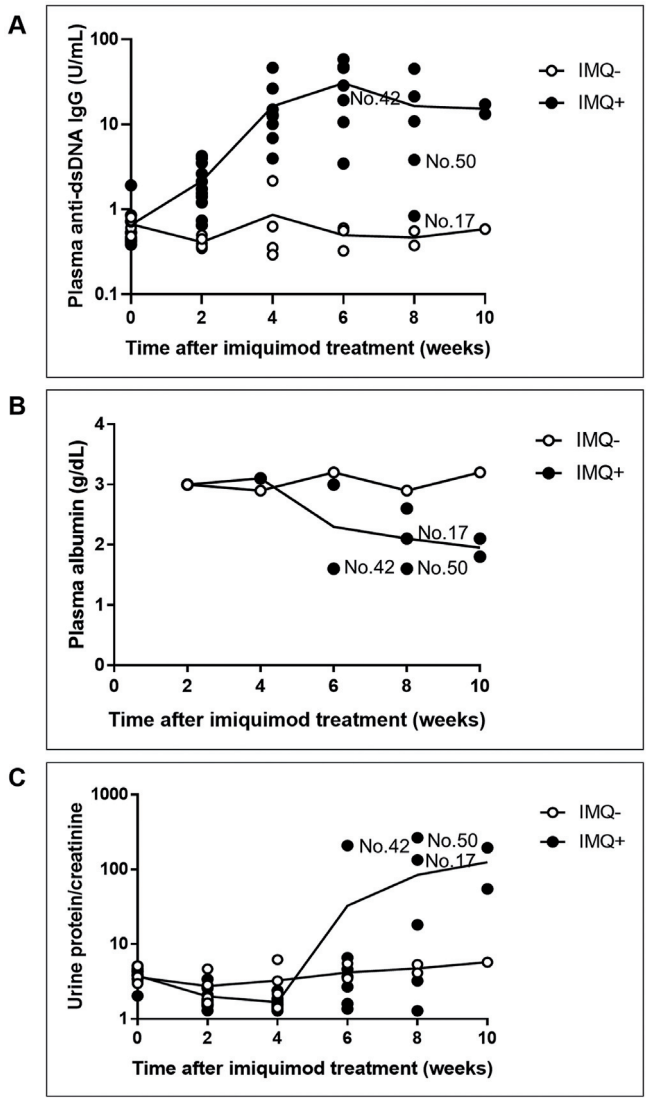

Fig. 1. Clinical parameters in Experiment 1. **A.** Plasma anti-dsDNA IgG. **B.** Plasma albumin. **C.** Urine protein/creatinine. Closed circles, IMQ-treated animals; open circles, control animals; lines, mean values of each group. Animal number indicates animals exhibiting podocyte vacuolation. IMQ, imiquimod.

nephrotic syndrome including proteinuria (Fig. 1C), decreased plasma albumin (Fig. 1B), cutaneous edema, and ascites (Table 1) showed podocyte vacuolation (Table 1, Fig. 2D,H) and podocyte decrease (Fig. 3C) as examined by IHC for p57 Kip2. An increase in anti-dsDNA IgG (Fig. 1A) seemed unrelated to the podocyte vacuolation.

Detailed analysis of glomeruli

In Experiment 2, glomeruli of mice at 8 weeks after IMQ treatment were analyzed. Using IF, mesangial deposits were observed in all animals treated with IMQ. IgG, IgA, IgM, and C1q were observed in all mice and C3 was observed in about 80% of mice (Fig. 4A,B).

Table 1. Results of histopathology and necropsy in experiment 1.

Weeks after IMQ treatment	4		6		8			10	
Animal No.	32	34	42	45	17	27	50	30	49
Histopathology									
Eosinophilic mesangial deposits	1	1	2	1	1	2	3	2	1
Enlargement of podocyte	-	-	P	-	P	P	P	P	P
Vacuolation of podocyte/PEC	-	-	P	-	P	-	P	-	-
Hypertrophy/hyperplasia of PEC	-	-	P	-	P	-	P	-	-
Necropsy									
Edema	-	-	P	-	-	-	P	-	-
Ascites	-	-	P	-	-	-	P	-	-

-, no abnormality; 1, minimal; 2, moderate; 3, severe; P, present, PEC: parietal epithelial cell. No abnormality was found in mice of both control and 2 weeks after IMQ treatment. n=2-3 imiquimod-treated and 1 control mouse at each point.

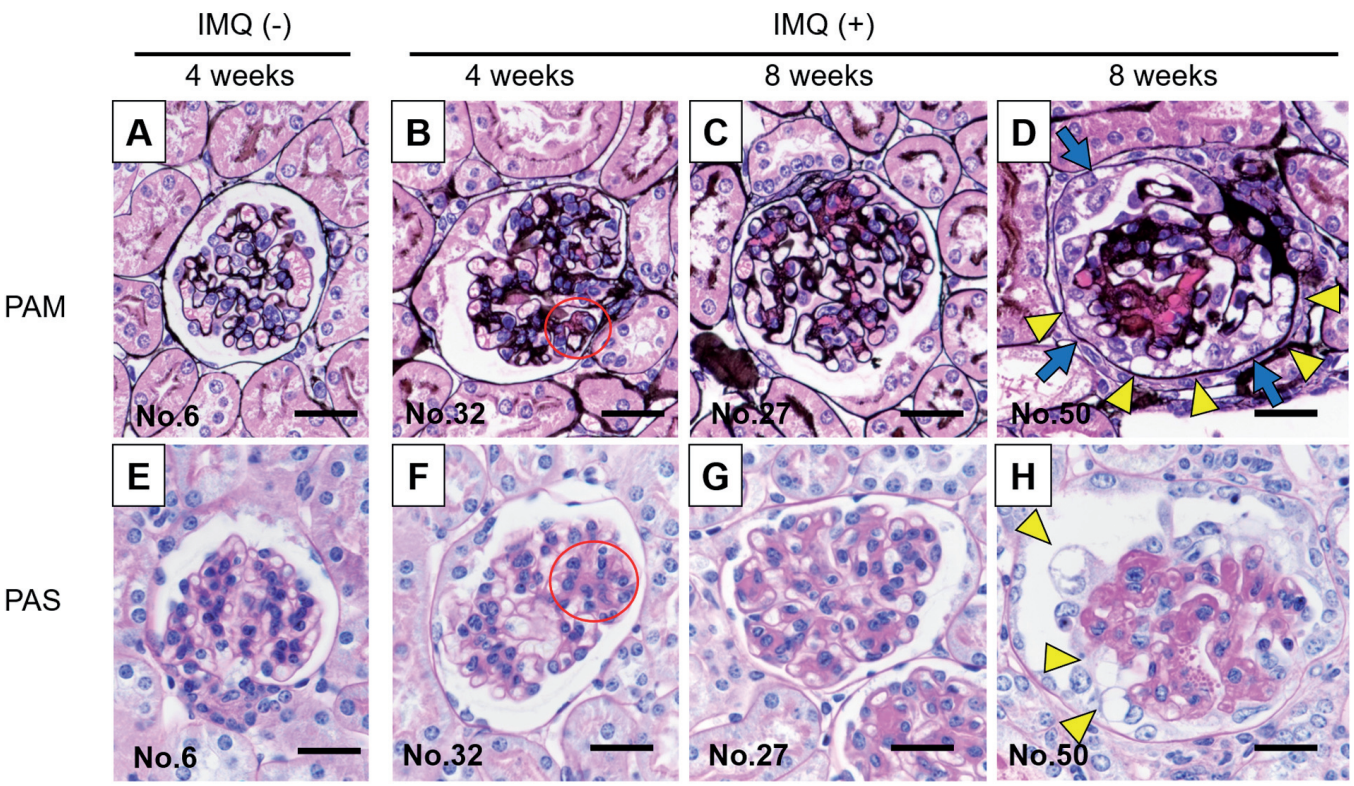

Fig. 2. Histopathology of glomeruli in Experiment 1. **A-D.** Periodic acid-methenamine silver stain. **E-H.** Periodic acid-schiff stain. The number indicates animal number. Segmental eosinophilic deposits (circle areas), vacuolation and enlargement of podocytes (arrowheads), and hypertrophy and hyperplasia with vacuolation of parietal epithelial cells (arrows). IMQ, imiquimod. Scale bars: 25 μm.

Deposits of all types of immunoglobulins including IgA, G, and M are characteristics of LN (Weening et al., 2004; Lech and Anders, 2013). According to IHC, inflammatory cells including CD3+ T cells, CD19+ B cells, F4/80+ macrophages, and Ly-6G+ neutrophils in glomeruli were not increased in IMQ-treated mice compared to those of control mice (Fig. 5A, Table 2). In contrast, infiltrated T cells and B cells were found around the arcuate artery (Fig. 5B) and/or renal pelvis in 80% of mice with IMQ treatment (data not shown).

TEM revealed electron-dense deposits in the mesangial area in IMQ-treated mice (Fig. 6E,H). In the case with severe proteinuria (Fig. 6J) and cytoplasmic vacuoles in podocytes (Fig. 6D,F), foot processes effacement (FPE) was observed by TEM (Fig. 6F). In the case without proteinuria (Fig. 6J), the foot processes were not effaced, but small cytoplasmic vacuoles were detected only by TEM (Fig. 6I). A few IC deposits were found in the glomerular basement membrane (GBM) using IF (Fig. 4B) and TEM (data not shown).

Table 2. Positive cell number per glomerulus.

	IMQ (-)	IMQ (+)
CD3	0.14±0.04	0.37±0.04
CD19	0.01±0.01	0.06±0.01
F4/80	0.00±0.00	0.02±0.01
Ly-6G	0.01±0.01	0.16±0.03

Values are mean ±SEM. P<0.05 IMQ (-) vs. IMQ (+) by Student's t-test. n=10 imiquimod-treated and 3 control mice.

Discussion

We have demonstrated that pathological features of kidney in IMQ-induced lupus mice correspond to those of class II LN in humans with podocyte injury. The first feature observed in all mice is mesangial deposits of all types of immunoglobulins, C3, and C1q without infiltration of inflammatory cells in glomeruli. In class II LN, subendothelial and subepithelial deposits are usually not detected by light microscopy; however, IF or electron microscopy can detect a few deposits (Weening et al., 2004). Taken together, our results show that IMQ-treated mice exhibit characteristics of class II LN. The second pathological feature, which was observed in some mice, is podocyte injury characterized by FPE, podocyte vacuolation and decrease. As FPE leads to severe proteinuria (Kopp et al., 2020), FPE is considered to induce proteinuria and nephrotic syndrome.

The location of IC deposits in glomeruli differs among classes of LN (Weening et al., 2004; Bajema et al., 2018). The deposits elicit renal damage through different mechanisms (Davidson, 2016). Subendothelial deposits, a characteristic of class III/IV LN, cause inflammatory responses due to complement activation by subendothelial deposits (Davidson, 2016; Sakhi et al., 2019). In class V LN, subepithelial deposits lead to podocyte injury, but inflammation is less severe than

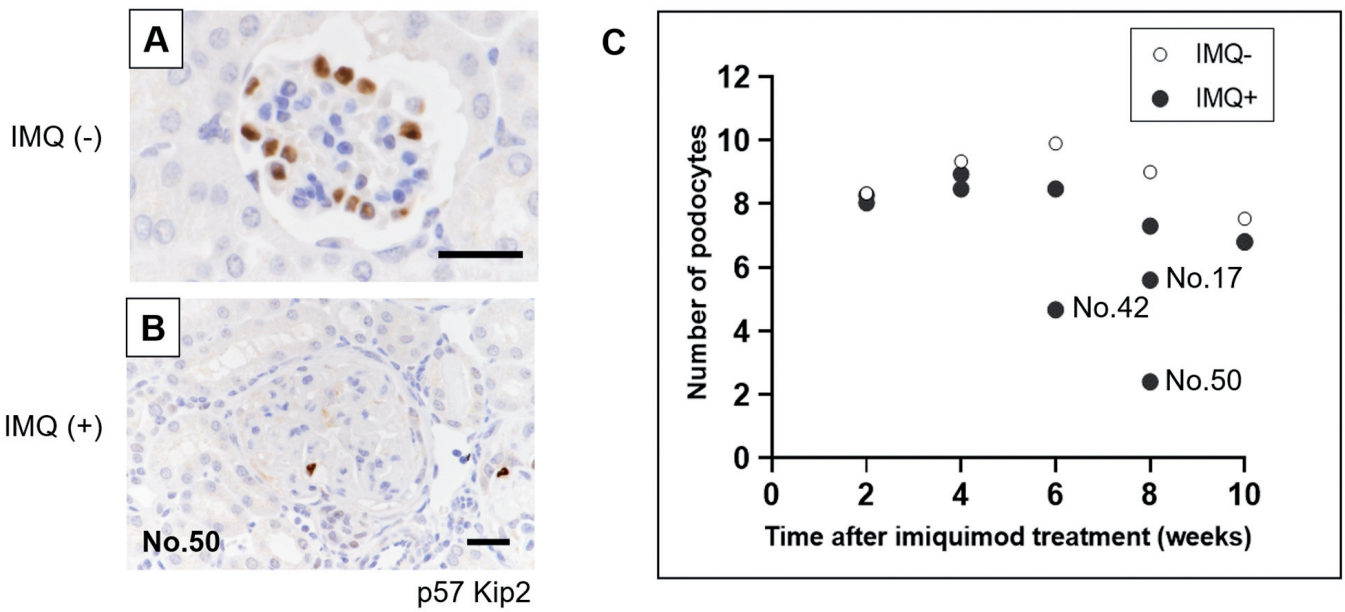

Fig. 3. Podocyte number in Experiment 1. **A, B.** Immunohistochemistry for p57 Kip2 of control mouse **(A)** and imiquimod-treated mouse **(B)**. **C.** Mean number of p57 Kip2-positive podocytes per glomerulus. Closed circles, IMQ-treated animals; open circles, control animals. Animal number indicates animals exhibiting podocyte vacuolation. IMQ, imiquimod. Scale bars: 25 μm.

that of class III/IV (Davidson, 2016; Sakhi et al., 2019; Gasparotto et al., 2020). The differences in deposits are associated with the quality of the autoantibodies that bind to antigens in glomeruli (Lech and Anders, 2013; Anders and Fogo, 2014; Sakhi et al., 2019). In humans, class III/IV LN occurs separately from class II or sequentially after class II (Anders and Fogo, 2014). Repeated biopsy of LN showed that about 80% of class II LN progress to a higher class, such as III, IV, or V (Narváez et al., 2017). Animal models of SLE usually develop class III/IV and develop inflammatory responses in glomeruli (Grande, 2011; Kimura et al., 2013). The shift from class II to III/IV LN is also known in NZB/W F1 mice, where decreased DNase I may lead to the accumulation of chromatin in GBM through the impaired fragmentation of chromatin (Pedersen et al., 2015). The present study showed that IMQ-treated FVB/N mice develop mesangial IC deposits without inflammatory cells in glomeruli, which is consistent with class II LN in humans (Weening et al., 2004). A limitation to our study is that it lasted only ten weeks, and therefore we could not determine whether the location remains unchanged or progresses to GBM, which would mean more severe classes, after prolonged treatment with IMQ. Podocyte injury makes longer treatment difficult because mice develop nephrotic syndrome. For a longer study, we may need to modify the experimental protocol, such as the IMQ dosage or administration frequency. In the IMQ-treated FVB/N mice, lymphocytes were found around arcuate arteries and/or the renal pelvis. A similar infiltration of cells reported in a mouse model of SLE has been described as "tertiary lymphoid structures" that work as lymph nodes in kidneys (Dorraji et al., 2020). The structures secrete autoantibody and contribute to local inflammation in SLE (Lech and Anders, 2013; Anders and Fogo, 2014; Dorraji et al., 2020).

TLR7 signaling is also activated in BXSB male mice, a spontaneous model of SLE. BXSB male mice have a y-linked autoimmune accelerating (Yaa) locus that encodes TLR7, which leads to about 2-fold increase in TLR7 transcription (Grande, 2011; Zhuang et al., 2015; Richard and Gilkeson, 2018). Interestingly, these mice develop membranous proliferative glomerulonephritis that corresponds to class III/IV LN (Kimura et al., 2013), whereas TLR7 activation in IMQ-treated mice results in class II LN. The different glomerular characteristics in IMQ-treated and BXSB male mice may be attributed to the manner of TLR7 activation or to the strains. The major target gene of Yaa- is TLR7, but other genes may be involved because TLR7 deletion does not halt autoantibody production (Fairhurst et al., 2008). It is possible that strain of mouse affects the severity of disease as induced by TLR7 activation. Compared with podocyte injury in the present IMQ-treated FVB/NJcl mice, podocyte injury in IMQ-treated C57BL/6 is milder, exhibiting only FPE and decreased expression of WT-1 and nephrin (Zhang et al., 2018). In addition, psoriasis-like lesions induced by IMQ treatment on skin are milder in C57BL/6 than those in BALB/c mice (van der Fits et al., 2009).

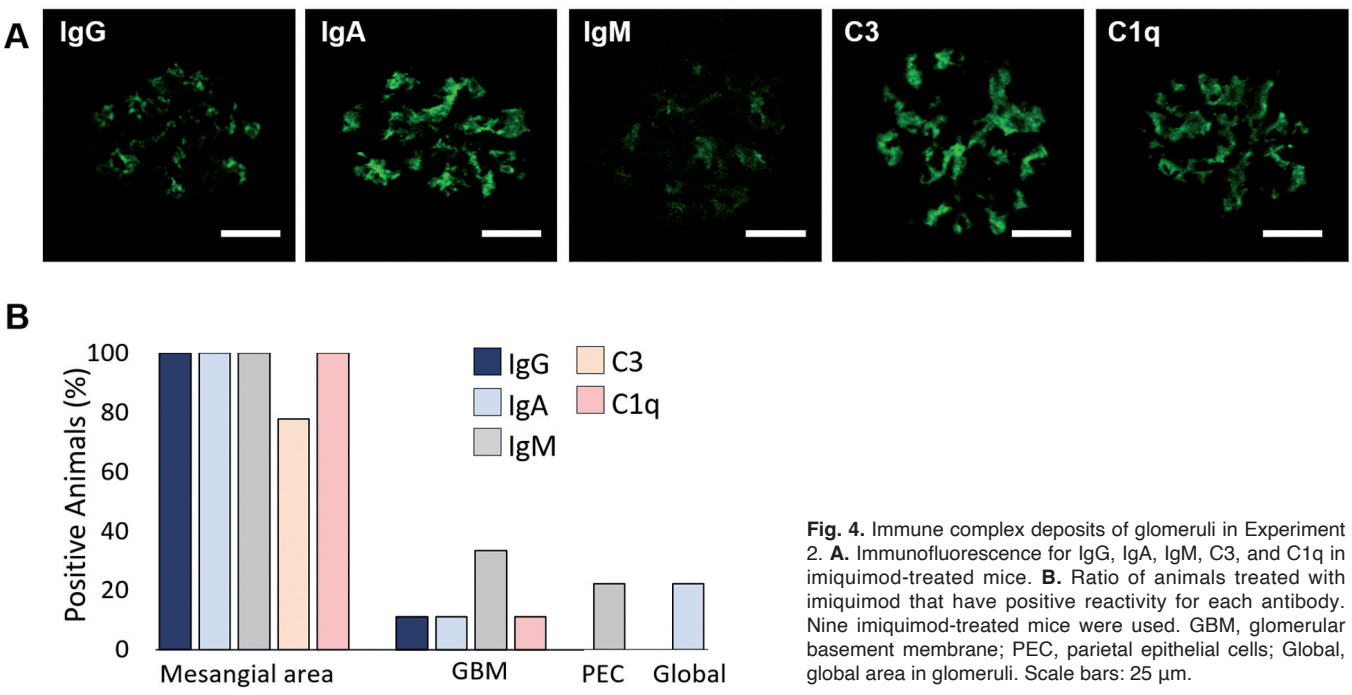

Fig. 4. Immune complex deposits of glomeruli in Experiment 2. **A.** Immunofluorescence for IgG, IgA, IgM, C3, and C1q in imiquimod-treated mice. **B.** Ratio of animals treated with imiquimod that have positive reactivity for each antibody. Nine imiquimod-treated mice were used. GBM, glomerular basement membrane; PEC, parietal epithelial cells; Global, global area in glomeruli. Scale bars: 25 μm.

Interestingly, the present study revealed IMQ-treated mice showed podocyte injury in 6 mice and exhibited nephrotic syndrome in 2 of these mice despite class II LN, where nephrotic syndrome is usually absent (Oliva-Damaso et al., 2019). Podocyte injury and nephrotic syndrome commonly occur in class III/IV and V LN because it is commonly related to endocapillary hypercellularity and IC deposits in glomerular capillary walls (Chen and Hu, 2018; Oliva-Damaso et al., 2019). On the other hand, recent studies have reported "lupus

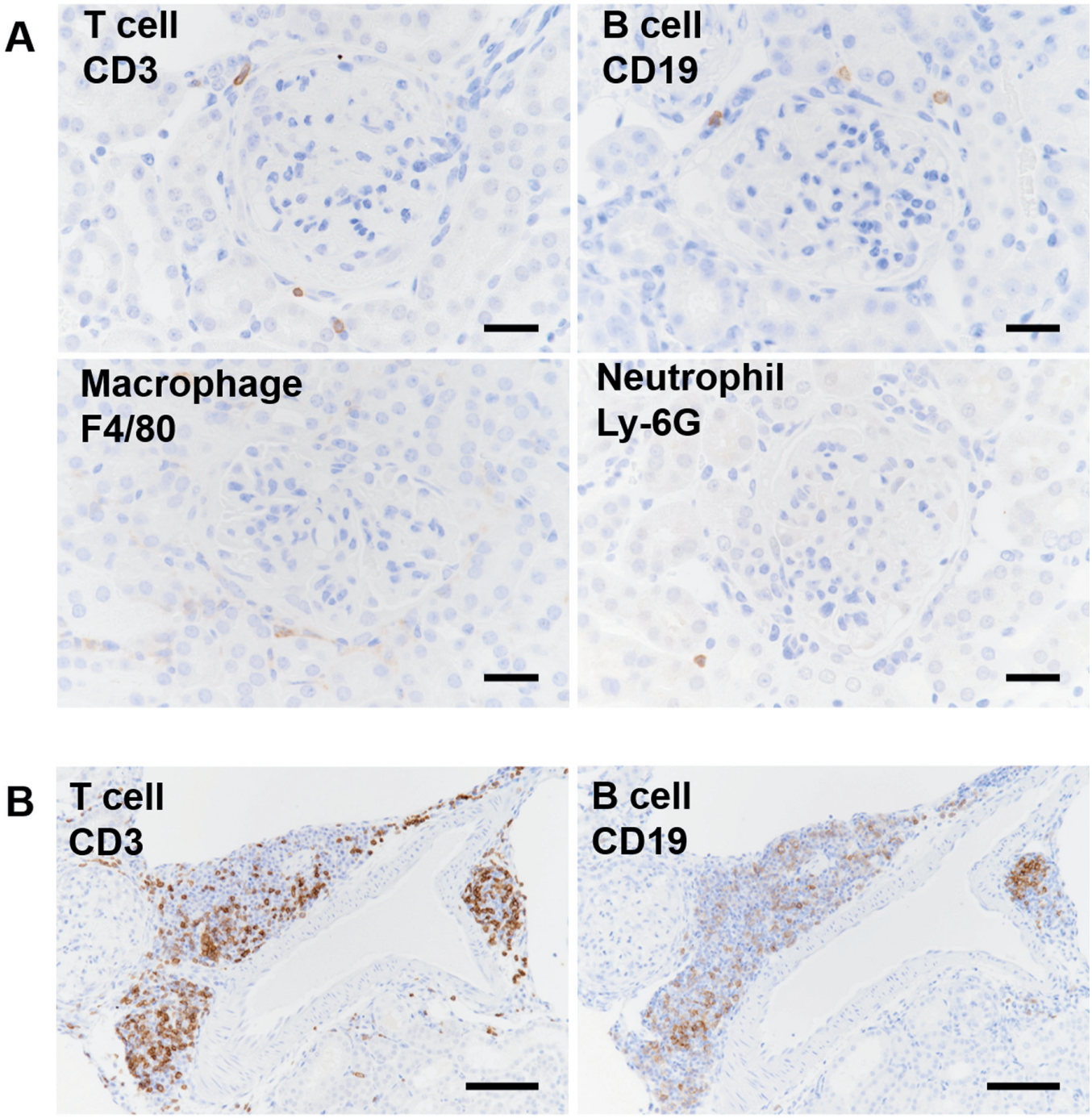

Fig. 5. Immunohistochemistry for inflammatory cells in Experiment 2. **A.** Immunohistochemistry for CD3, CD19, F4/80, and Ly-6G in glomeruli of imiquimod-treated mice. **B.** Immunohistochemistry for CD3 and CD19 around arcuate arteries of kidney. Scale bars: A, 25 μm; B, 100 μm.

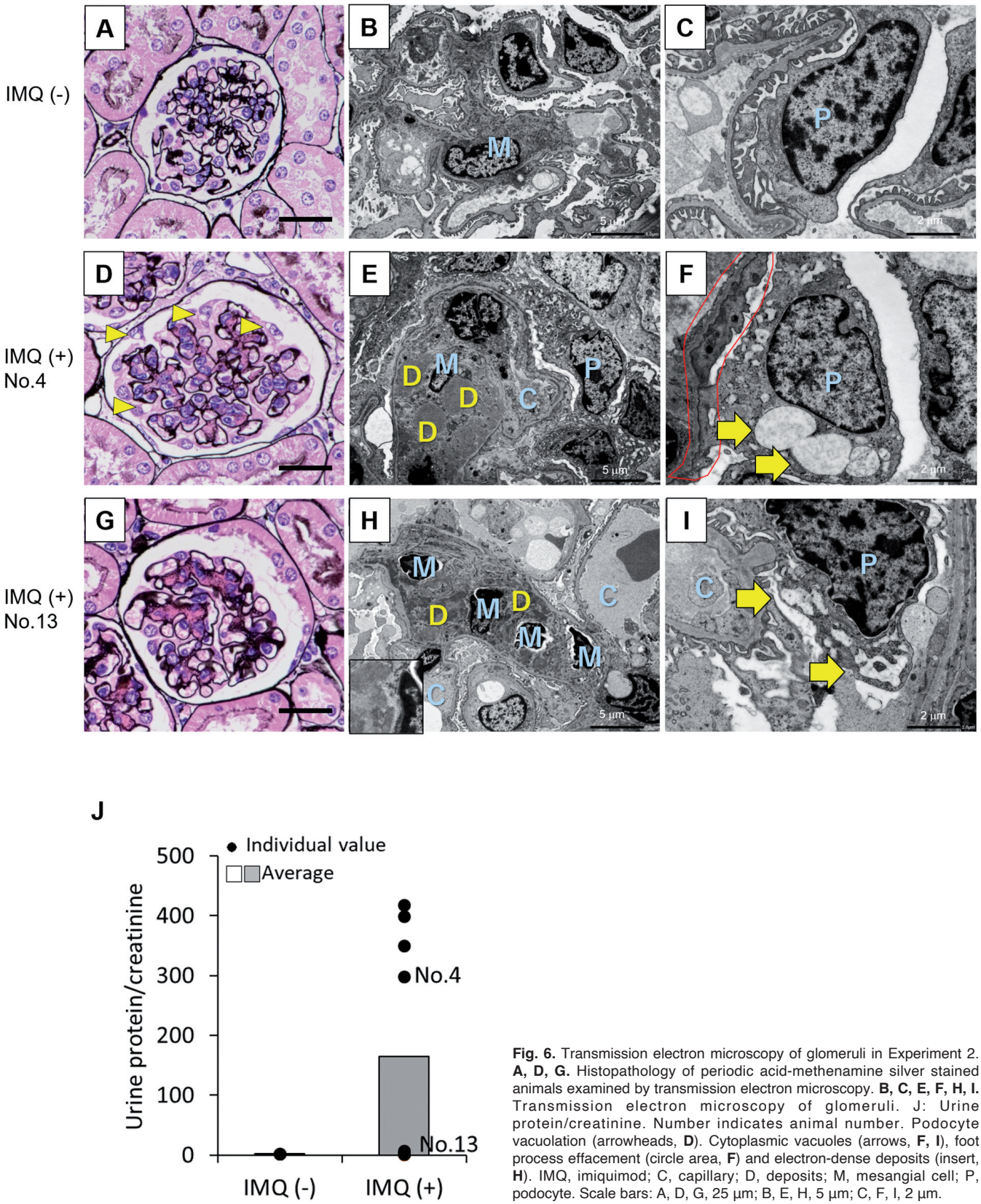

Fig. 6. Transmission electron microscopy of glomeruli in Experiment 2. **A, D, G.** Histopathology of periodic acid-methenamine silver stained animals examined by transmission electron microscopy. **B, C, E, F, H, I.** Transmission electron microscopy of glomeruli. J: Urine protein/creatinine. Number indicates animal number. Podocyte vacuolation (arrowheads, **D**). Cytoplasmic vacuoles (arrows, **F, I**), foot process effacement (circle area, **F**) and electron-dense deposits (insert, **H**). IMQ, imiquimod; C, capillary; D, deposits; M, mesangial cell; P, podocyte. Scale bars: A, D, G, 25 μm; B, E, H, 5 μm; C, F, I, 2 μm.

podocytopathy" that is a distinct form of LN and is not applicable to any ISN/RPS classification. Nephrotic syndrome occurs >90% in patients with lupus podocytopathy; this proportion is higher than any class of ISN/RPS classification (Oliva-Damaso et al., 2019; Sakhi et al., 2019). Lupus podocytopathy is confirmed by the presence of diffuse FPE by electron microscopy without subendothelial or subepithelial IC deposits, and has characteristics of classes I or II LN, minimal change disease, or focal segmental glomerulosclerosis (FSGS). It affects about 1% of LN patients and is accompanied clinically by severe proteinuria (Chen and Hu, 2018; Oliva-Damaso et al., 2019; Sakhi et al., 2019; Gasparotto et al., 2020). Podocyte injury is considered to be induced by cytokines, lymphokines, or T cell dysfunction, but not by immune deposits (Chen and Hu, 2018; Oliva-Damaso et al., 2019; Kopp et al., 2020).

Cytokines including TNF-α, IFN-γ, IL-6, and IL-10 are released from dendritic cells after treatment with IMQ (Gong et al., 2014). Cytokines such as TNF-α and TGF-β1 are also released by mesangial cells in IgA nephropathy and cause podocyte damage (Trimarchi and Coppo, 2019). Complement membrane attack complex deposits induce TGF-β1 and IL-6 production by mesangial cells in a Thy-1 nephritis model (Zhang et al., 2014). The present study showed that podocyte injury develops after mesangial deposits appear. Thus, it is possible that mesangial cells contribute to the development of podocyte injury by secreting cytokines in local areas. Another possibility is that IMQ, a TLR7 ligand, binds directly to podocytes. TLR8 is known to be expressed in podocytes and TLR8 activation with IL-1β causes podocyte injury in mice with unilateral ureteral obstruction (Masum et al., 2021). TLR4 is consistently expressed in podocytes and leads to membrano-proliferative glomerulonephritis in mice by releasing chemokines (Banas et al., 2008). In contrast, TLR7 expression is restricted to dendritic cells and macrophages, and B cells (Eleftheriadis et al., 2012; Lech and Anders, 2013; Zhuang et al., 2015) and is not reported in podocytes. Thus, we think that podocyte injury in the IMQ-induced model is not caused by TLR7 ligands, but rather by plasma factors produced by immune cells or mesangial cells. Further studies are needed to elucidate the exact mechanisms of podocyte injury.

In conclusion, we demonstrated that IMQ-induced kidney lesions in female FVB/NJcl wild type mice correspond to class II LN, and are characterized by polyclonal mesangial deposits without infiltration of inflammatory cell in glomeruli. It is accompanied by podocyte injury leading to nephritic syndrome. These characteristics are distinct from other mouse models of SLE. The present model is useful for research on LN; for example, by allowing researchers to investigate the mechanisms of IC deposits through comparison with other mouse models, or to investigate how podocyte injury develops independently of IC deposits.

Acknowledgements. The present work was supported by Chugai Research Institute for Medical Science, Inc. and Kazuki Ohtake.
A conflict of interest statement. The authors declare no conflicts of interest associated with this manuscript.

References

Anders H.J. and Fogo A.B. (2014). Immunopathology of lupus nephritis. Semin. Immunopathol. 36, 443-459.

Bajema I.M., Wilhelmus S., Alpers C.E., Bruijn J.A., Colvin R.B., Cook H.T., D'Agati V.D., Ferrario F., Haas M., Jennette J.C., Joh K., Nast C.C., Noël L.H., Rijnink E.C., Roberts I.S.D., Seshan S.V., Sethi S. and Fogo A.B. (2018). Revision of the international society of nephrology/renal pathology society classification for lupus nephritis: Clarification of definitions, and modified national institutes of health activity and chronicity indices. Kidney Int. 93, 789-796.

Banas M.C., Banas B., Hudkins K.L., Wietecha T.A., Iyoda M., Bock E., Hauser P., Pippin J.W., Shankland S.J., Smith K.D., Stoelcker B., Liu G., Gröne H.J., Krämer B.K. and Alpers C.E. (2008). TLR4 links podocytes with the innate immune system to mediate glomerular injury. J. Am. Soc. Nephrol. 19, 704-713.

Chen D. and Hu W. (2018). Lupus podocytopathy: A distinct entity of lupus nephritis. J. Nephrol. 31, 629-634.

Davidson A. (2016). What is damaging the kidney in lupus nephritis?. Nat. Rev. Rheumatol. 12, 143-153.

Dorraji S.E., Kanapathippillai P., Hovd A.K., Stenersrød M.R., Horvei K.D., Ursvik A., Figenschau S.L., Thiyagarajan D., Fenton C.G., Pedersen H.L. and Fenton K.A. (2020). Kidney tertiary lymphoid structures in lupus nephritis develop into large interconnected networks and resemble lymph nodes in gene signature. Am. J. Pathol. 190, 2203-2225.

Eleftheriadis T., Pissas G., Liakopoulos V., Stefanidis I. and Lawson B.R. (2012). Toll-like receptors and their role in renal pathologies. Inflamm. Allergy Drug Targets 11, 464-477.

Fairhurst A.M., Hwang S.H., Wang A., Tian X.H., Boudreaux C., Zhou X.J., Casco J., Li Q.Z., Connolly J.E. and Wakeland E.K. (2008). Yaa autoimmune phenotypes are conferred by overexpression of TLR7. Eur. J. Immunol. 38, 1971-1978.

Gasparotto M., Gatto M., Binda V., Doria A. and Moroni G. (2020). Lupus nephritis: Clinical presentations and outcomes in the 21st century. Rheumatology (Oxford) 59, v39-v51.

Gong L., Wang Y., Zhou L., Bai X., Wu S., Zhu F. and Zhu Y.F. (2014). Activation of toll-like receptor-7 exacerbates lupus nephritis by modulating regulatory T cells. Am. J. Nephrol. 40, 325-344.

Grande J.P. (2011). Experimental models of lupus nephritis. Contrib. Nephrol.169, 183-197.

Kimura J., Ichii O., Otsuka S., Sasaki H., Hashimoto Y. and Kon Y. (2013). Close relations between podocyte injuries and membranous proliferative glomerulonephritis in autoimmune murine models. Am. J. Nephrol. 38, 27-38.

Kopp J.B., Anders H.J., Susztak K., Podestà M.A., Remuzzi G., Hildebrandt F. and Romagnani P. (2020). Podocytopathies. Nat. Rev. Dis. Primers 6, 68.

Lech M. and Anders H.J. (2013). The pathogenesis of lupus nephritis. J. Am. Soc. Nephrol. 24, 1357-1366.

Maeda A., Fukushima N., Horiba N., Segawa H. and Miyamoto K.I. (2019). The role of extracellular phosphate levels on kidney disease

progression in a podocyte injury mouse model. Nephron 142, 135-146.

Masum M.A., Ichii O., Elewa Y.H.A. and Kon Y. (2021). Podocyte injury through interaction between tlr8 and its endogenous ligand mir-21 in obstructed and its collateral kidney. Front. Immunol. 11, 606488.

Moroki T., Matsuo S., Hatakeyama H., Hayashi S., Matsumoto I., Suzuki S., Kotera T., Kumagai K. and Ozaki K. (2021). Databases for technical aspects of immunohistochemistry: 2021 update. J. Toxicol. Pathol. 34, 161-180.

Narváez J., Ricse M., Gomà M., Mitjavila F., Fulladosa X., Capdevila O., Torras J., Juanola X., Pujol-Farriols R. and Nolla J.M. (2017). The value of repeat biopsy in lupus nephritis flares. Medicine (Baltimore) 96, e7099.

Oliva-Damaso N., Payan J., Oliva-Damaso E., Pereda T. and Bomback A.S. (2019). Lupus podocytopathy: An overview. Adv. Chronic Kidney Dis. 26, 369-375.

Pawar R.D., Patole P.S., Zecher D., Segerer S., Kretzler M., Schlöndorff D. and Anders H.J. (2006). Toll-like receptor-7 modulates immune complex glomerulonephritis. J. Am. Soc. Nephrol. 17, 141-149.

Pedersen H.L., Horvei K.D., Thiyagarajan D., Seredkina N. and Rekvig O.P. (2015). Murine and human lupus nephritis: Pathogenic mechanisms and theoretical strategies for therapy. Semin. Nephrol. 35, 427-438.

Richard M.L. and Gilkeson G. (2018). Mouse models of lupus: What they tell us and what they don't. Lupus Sci. Med. 5, e000199.

Sakata K., Nakayamada S., Miyazaki Y., Kubo S., Ishii A., Nakano K. and Tanaka Y. (2018). Up-regulation of TLR7-mediated IFN-α production by plasmacytoid dendritic cells in patients with systemic lupus erythematosus. Front. Immunol. 9, 1957.

Sakhi H., Moktefi A., Bouachi K., Audard V., Hénique C., Remy P., Ollero M. and El Karoui K. (2019). Podocyte injury in lupus nephritis. J. Clin. Med. 8, 1340.

Satoh M., Kumar A., Kanwar Y.S. and Reeves W.H. (1995). Anti-nuclear antibody production and immune-complex glomerulonephritis in balb/c mice treated with pristane. Proc. Natl. Acad. Sci. USA 92, 10934-10938.

Trimarchi H. and Coppo R. (2019). Podocytopathy in the mesangial proliferative immunoglobulin a nephropathy: New insights into the mechanisms of damage and progression. Nephrol. Dial. Transplant. 34, 1280-1285.

van der Fits L., Mourits S., Voerman J.S., Kant M., Boon L., Laman J.D., Cornelissen F., Mus A.M., Florencia E., Prens E.P. and Lubberts E. (2009). Imiquimod-induced psoriasis-like skin inflammation in mice is mediated via the il-23/il-17 axis. J. Immunol. 182, 5836-5845.

Weening J.J., D'Agati V.D., Schwartz M.M., Seshan S.V., Alpers C.E., Appel G.B., Balow J.E., Bruijn J.A., Cook T., Ferrario F., Fogo A.B., Ginzler E.M., Hebert L., Hill G., Hill P., Jennette J.C., Kong N.C., Lesavre P., Lockshin M., Looi L.M., Makino H., Moura L.A. and Nagata M. (2004). The classification of glomerulonephritis in systemic lupus erythematosus revisited. Kidney Int. 65, 521-530.

Yokogawa M., Takaishi M., Nakajima K., Kamijima R., Fujimoto C., Kataoka S., Terada Y. and Sano S. (2014). Epicutaneous application of toll-like receptor 7 agonists leads to systemic autoimmunity in wild-type mice: A new model of systemic lupus erythematosus. Arthritis Rheumatol. 66, 694-706.

Zhang J., Li Y., Shan K., Wang L., Qiu W., Lu Y., Zhao D., Zhu G., He F. and Wang Y. (2014). Sublytic C5b-9 induces IL-6 and TGF-β1 production by glomerular mesangial cells in rat Thy-1 nephritis through p300-mediated C/EBPβ acetylation. FASEB J. 28, 1511-1525.

Zhang D., Xu J., Ren J., Ding L., Shi G., Li D., Dou H. and Hou Y. (2018). Myeloid-derived suppressor cells induce podocyte injury through increasing reactive oxygen species in lupus nephritis. Front. Immunol. 9, 1443.

Zhuang H., Szeto C., Han S., Yang L. and Reeves W.H. (2015). Animal models of interferon signature positive lupus. Front. Immunol. 6, 291.

Accepted March 17, 2022